Multi-Frequency Mutation Detection in Broadband Electronic Signals Using SVD Denoising, Improved Mask EMD, and PSO-Optimized SVM

Qingfeng Yao
Anhui Business and Technology College, Intelligent Manufacturing and Automotive College, Hefei 231131, China
E-mail: qfeng115@126.com

Keywords: complex communication environment, multi-frequency mutation detection, singular value decomposition, improved mask emd decomposition, hilbert transform, PSO-SVM model

Received: March 13, 2025

When wideband electronic signals undergo multi-frequency mutations, the mutation times, amplitudes and phase changes of each frequency component are different, making it extremely difficult to accurately distinguish the characteristics of the mutated signals from the complex signal background. To this end, a detection method integrating the improved mask EMD and PSO-SVM is proposed. The singular value decomposition method is adopted to denoise wideband electronic signals, and the steady-state components and abrupt components of the signals are analyzed. The improved mask EMD method is adopted to extract the intrinsic modal function components of each order, extract the multi-frequency instantaneous frequencies and instantaneous energies of the corresponding components of the wideband electronic signal, construct the multi-frequency mutation feature set, and input it into the PSO-SVM detection model to capture the steady-state components and mutation components in the signal, and realize the multi-frequency mutation detection of wideband electronic signals. The experimental results show that the research method adopts the combined processing of improved mask and EMD, which reduces the signal reconstruction error compared with the traditional EMD method and eliminates the modal aliasing phenomenon. Combined with the SVM classifier optimized by PSO, the F1-score reached 0.92 on the same test set, which was significantly better than the machine learning non-orthogonal signal detection method. The indicators such as the instantaneous bandwidth (12.58Hz), frequency resolution (0.18Hz) and dynamic range (100dB) of this method are all superior to those of the baseline method, providing an effective solution for the detection of sudden changes in broadband signals in complex communication environments.

Povzetek: Za zaznavanje sprememb v širokopasovnih elektronskih signalih v zapletenih komunikacijskih okoljih je razvita metoda, ki združuje razširjeno maskirano empirično razcepno metodo (improved mask EMD), singularno vrednostno dekompozicijo za odstranjevanje šuma ter model podpore vektorjev, optimiziran z delčnim rojem (PSO-SVM). Metoda učinkovito loči stabilne in mutirajoče komponente signala ter omogoča kvalitetno zaznavanje večfrekvenčnih sprememb v hrupnih širokopasovnih sistemih.

1 Introduction

With the rapid change of information technology, wireless communication technology plays an increasingly important role in national economy, national defense construction, scientific research and other fields [1]. However, in the actual communication process, the signal transmission environment presents a high degree of complexity and variability, not only the type and number of signals climbing dramatically, the mutual interference between the signals is also increasingly prominent [2]. Especially in the broadband communication system, due to the significant expansion of the signal bandwidth, the multi-frequency mutation phenomenon of the signal becomes particularly prominent. This kind of signal is famous for the complexity of frequency components, the rapidity of the change speed and the short duration, which undoubtedly greatly increases the difficulty of signal processing, and may also pose a serious challenge to the stability and reliability of the communication system. Therefore, in-depth exploration and study of broadband electronic signal multi-frequency mutation detection methods applicable to complex communication environments is not only of far-reaching significance for improving the overall performance of communication systems, but also an indispensable part of guaranteeing the quality of information transmission and promoting the continuous progress of wireless communication technology [3].

In recent years, scholars at home and abroad have achieved certain research results in multi-frequency mutation detection of broadband electronic signals. Yldrm trains a deep learning model that can detect signals by deep learning OFDM-AIM signals. Then the signal to be detected is inputted into the model and the signal detection results are output, and then the intermediate results or parameters of pre-calculation are stored by using look-up tables, the parameters are optimized by using the taboo search algorithm, and the parallel processing is adopted to accelerate the calculation process and improve the signal detection efficiency. Deep learning models may only be exposed to a limited number of signal patterns during the training stage. However, in a complex communication environment, the multi-frequency sudden change characteristics of signals may exceed the training range of the model, and it is difficult for the model to fully learn all possible feature combinations. Furthermore, when the lookup table is confronted with a large number of mutation signals, its storage and retrieval efficiency may be severely affected, and it is difficult to cover all possible mutation situations [4]. Kulkarni et al. use deep learning and other techniques for feature extraction and pattern recognition of wireless signals, and at the same time, combined with approximation computation techniques, to reduce the computational complexity and energy consumption under the premise of ensuring that the detection accuracy meets the needs of the application. Approximate computing technology is achieved by sacrificing some accuracy. When dealing with multi-frequency abrupt change signals, this approximate calculation may lead to the loss of key feature information, making it difficult for the model to accurately distinguish the true abrupt change signal features [5]. Baek et al. use FTN technology to transmit higher rate non-orthogonal signals at the transmitter side, and use the DBN-SVM model at the receiver side to perform anomalous feature extraction and pattern recognition on the received signals. When the DDBN-SVM model is confronted with such complex ISI and variable multi-frequency mutation signals, it cannot fully consider all possible ISI and multi-frequency mutation combinations during training, resulting in a decrease in the recognition accuracy of mutation signal features in practical applications [6]. Meier et al. used acousto-optic frequency modulation and other technical means to achieve high-speed, highly linear and continuous step frequency modulation inside a fiber optic loop, so as to generate ultra-wideband radar signals by using low-speed electronic signals, and then realize the detection of high-bandwidth arbitrary signals. This method itself may introduce noise and distortion during the signal conversion and transmission process. Multi-frequency abrupt change signals will further intensify this interference, increase the difficulty of feature extraction and resolution, and it is difficult to capture the detailed variation information of each frequency component [7].

Aiming at the problem of multi-frequency mutation detection of broadband electronic signals in complex communication environments, this study focuses on solving the following three key scientific issues:

(1) How to improve the mask EMD method to significantly reduce the modal aliasing phenomenon in the IMF decomposition of wideband signals?

(2) Under the condition of strong noise interference, how to effectively extract and distinguish the steady-state components and abrupt components of broadband signals?

(3) How to construct a detection model with strong robustness to improve the recognition accuracy of multi-frequency abrupt change signals?

Based on these problems, this paper proposes a detection method that integrates the improved mask EMD and PSO-SVM.

The Singular Value Decomposition (SVD) is adopted to preprocess the wideband electronic signal, effectively suppressing the interference of complex environmental noise. By analyzing the characteristic differences between the steady-state and mutant components of the signal, an improved mask EMD method was proposed, which significantly improved the modal aliasing problem of IMF components. The Hilbert transform was utilized to extract the characteristics of multi-frequency instantaneous frequencies and instantaneous energies, and an SVM detection model based on PSO optimization was constructed, achieving the accurate identification of multi-frequency abrupt components in wideband electronic signals. The experimental results show that this method is superior to the existing technologies in key indicators such as instantaneous bandwidth and frequency resolution.

2 Broadband electronic signal multi-frequency mutation detection

2.1 SVD-based denoising of broadband electronic signals for complex communication environments

In the complex communication environment, broadband electronic signals are subject to multiple threats such as same-frequency interference, neighboring-frequency interference, intermodulation interference and thermal noise, scattering noise, scintillation noise, etc. These interferences and noises are easy to trigger changes in the signal spectra [8], which lead to sudden changes in the frequency components during the transmission process. In order to improve the reliability and accuracy of signal transmission, it is crucial to detect multi-frequency mutations in broadband electronic signals. Through effective denoising of broadband electronic signals in complex communication environments, the influence of interference and noise can be significantly reduced or eliminated, so that the multi-frequency mutation characteristics of broadband electronic signals are more clearly discernible, and the accurate capture and identification of frequency mutation components can be realized [9], which improves the accuracy and efficiency of the multi-frequency mutation detection, and provides a solid guarantee for the stable operation of the communication system. The singular value decomposition (SVD) method removes the noise and unnecessary components of broadband electronic signals by decomposing the broadband electronic signal matrix and filtering and truncating the singular values in the matrix.

For noise-contaminated broadband electronic signals $\overline{X} = \{\overline{x}_1, \overline{x}_2, \cdots, \overline{x}_L\}$ in complex communication environments, constructed into a $m \times n(m \le n)$ dimensional Hankel matrix given by:

$$A_{m\times n} \equiv \begin{bmatrix} \overline{x}_1 & \overline{x}_2 & \cdots \overline{x}_n \\ \overline{x}_2 & \overline{x}_3 & \cdots \overline{x}_{n+1} \\ \vdots & \vdots & \vdots \quad \vdots \\ \overline{x}_m & \overline{x}_{m+1} & \cdots \overline{x}_L \end{bmatrix} \tag{1}$$

Of which, A is the Hankel matrix; the embedding dimension is denoted by m ; the number of signal sampling points is n and is satisfied $m+n-1=L$.

A singular value decomposition of the Hankel matrix yields:

$$A = U\Sigma V^T \tag{2}$$

Of which, U is $m\times m$ dimensional orthogonal matrices; V is $n\times n$ dimensional orthogonal matrices; Σ is $m\times n$ dimensional matrix. The main diagonal elements are the singular values of the matrix and are arranged in descending order.

Matrix A is the Hankel matrix composed of the noise-contaminated broadband electronic signals, which can be expressed as the sum of the subspace of the uncontaminated broadband electronic signals and the subspace of the noise, and is computed as:

$$A = \overline{A} + N = [U_r U_0]\begin{pmatrix} \Sigma_r & 0 \\ 0 & \Sigma_0 \end{pmatrix}\begin{bmatrix} V_r^T \\ V_0^T \end{bmatrix} \tag{3}$$

Of which: $\overline{A}$ is the subspace of broadband electronic signals uncontaminated by noise; N is the noise subspace. Noise reduction of the original broadband electronic signal translates into the known A , looking for the best approximation of $\overline{A}$, The better the approach degree, the more obvious the noise reduction effect is [10].

The first k effective singular values of the diagonal matrix are preserved, and the other singular values are set to zero, the reconstructed matrix is obtained by using the inverse process of singular value decomposition. Generally speaking, the reconstruction matrix is no longer in the form of Hankel matrix. In order to obtain the width of the electronic signal after noise reduction, it is necessary to average the elements of the reconstruction matrix with the following formula:

$$x_i = \frac{1}{o-l+1}\sum_{j=1}^{o}\overline{A}_{i-j+1,j} \tag{4}$$

Of which: i represents the index value in the reconstructed signal sequence; l 、 o intermediate variables used for summing the boundaries of the range, $l = \max(1, i-m+1)$, $o = \min(n,i)$; j represents the loop variable of the summation operation.

$X = \{x_1, x_2, \cdots, x_L\}$ which is composed by x_i , that is, the broadband electronic signal after noise reduction.

SVD can decompose the broadband electronic signal matrix into the product form of the left singular matrix, the singular value matrix and the right singular matrix. The noise in the signal is usually reflected in the components corresponding to smaller singular values. The denoising purpose can be achieved by processing the singular values. Since most of the smaller singular values correspond to the noise components, truncating these singular values can effectively remove the noise, but at the same time, it may also cause some signal information loss. As for the selection of the optimal cut-off point, different truncation positions are attempted, and factors such as the improvement degree of SNR of the signal after noise reduction, the size of the mean square error, and the retention of signal characteristics are comprehensively considered. For example, if a higher noise reduction level is pursued, more singular values might be truncated, but this may lead to an increase in signal information loss; If more attention is paid to preserving the details of the signal, the number of truncated singular values should be appropriately reduced, and a trade-off should be made between noise reduction and signal information loss to determine the optimal cut-off point, so that the denoised signal can retain the key information of the original signal to the greatest extent while meeting certain noise reduction requirements.

2.2 Analysis of steady state and mutation components of broadband electronic signals

The steady state component reflects the inherent characteristics of the signal in a relatively stable state, such as the frequency distribution and amplitude characteristics of the normal mode of operation, and provides the basis for understanding the regular performance of the signal. By accurately grasping the steady state component, the normal model of the signal can be constructed as a reference standard for judging the occurrence of mutation. The mutation component, on the other hand, directly reflects the abnormal changes of the signal, and is the core concern of multi-frequency mutation detection. Analyzing the mutation components can clarify the time of the mutation, the frequency range involved, the magnitude of the mutation and other key parameters, which can help to understand the nature and characteristics of the mutation. By combining the two analyses, multi-frequency mutation phenomena can be accurately identified in complex broadband electronic signals, providing powerful support for subsequent signal processing, fault diagnosis, target detection and other applications. Therefore, before the multi-frequency mutation detection of broadband electronic signals, it is necessary to clarify the meanings and differences between the steady state components and the mutation components in broadband electronic signals. In order to explain the difference between these two components as easily as possible, the statistical probability and the difference information will be considered comprehensively. From the point of view of statistical probability theory, the steady state component can be regarded as a kind of component that appears in broadband electronic signals from the beginning to the end, while the mutation component is a kind of component that appears episodically in broadband electronic signals, and the two kinds of components can be expressed in the form of Equation (5), and Equation (6), respectively, in which P_s and P_m denote the frequency of occurrence of the steady state component and the mutant component in the broadband electronic signal, respectively.

$$P_s \approx 1 \tag{5}$$

$$P_s \otimes P_m \tag{6}$$

From the point of view of difference information theory, there are obvious differences in attribute characteristics between the steady state components and the mutation components, and these differences can then be recognized that these two components belong to different kinds rather than fluctuations in attribute characteristics between components in the same kind, which can be expressed in the form of equation (7), in the formula, $F(\cdot)$ denotes a method for obtaining attribute characteristics of broadband electronic signal components. X_s and X_m denote the steady-state and mutation components of the broadband electronic signal, respectively. δ is the critical value of the difference between the two components in terms of certain attribute characteristics, the value of which needs to be determined according to the specific attribute characteristics.

$$F(X_s) - F(X_m) > \delta \tag{7}$$

By combining these two theories to consider the components of broadband electronic signals, the meaning and difference between the steady state components and the mutation components can be further understood. According to the meaning and difference of these two components, the detection of multi-frequency mutation components of broadband electronic signals can be realized. In this paper, we extract the multifrequency instantaneous frequencies and instantaneous energies of broadband electronic signals and input them as feature quantities into the PSO-SVM-based detection model to realize the detection of multifrequency mutations of broadband electronic signals.

2.3 Broadband electronic signal decomposition based on improved mask EMD

EMD decomposition of denoised broadband electronic signals can help detect and analyze multi-frequency mutations in signals by revealing the time-dependent characteristics of the signals on different time scales and frequency components [11]. However, the decomposition of broadband electronic signals using the EMD method suffers from modal aliasing [12], i.e., signals with different frequency components may interfere with each other, resulting in inaccurate decomposition results. Therefore, this paper adopts the improved mask EMD method to process the denoised broadband electronic signals, aiming at effectively suppressing the modal aliasing phenomenon and improving the accuracy and reliability of the signal decomposition through the introduction of mask signals. The improved mask signal generation process is as follows:

(1) The denoised broadband electronic signal is denoted by $x(t)$, creating an improved mask signal $s(t)$, through the calculation with $x(t)$, the new signal $x_+(t)$ and $x_-(t)$ can be obtained:

$$\begin{cases} x_+(t) = x(t) + s(t) \\ x_-(t) = x(t) - s(t) \end{cases} \tag{8}$$

(2) EMD decomposition was performed to $x_+(t)$ and $x_-(t)$ to obtain the intrinsic modal functions $h_+(t)$ and $h_-(t)$, respectively.

(3) The IMF_1 component of the denoised broadband electronic signal $x(t)$ is:

$$h(t) = 2^{-1}\left[h_+(t) + h_-(t)\right] \tag{9}$$

Where: the analytical time of the intrinsic modal function is expressed as t.

Repeating steps (1)-(3) continuously, the IMF components and residuals of each order can be obtained, namely:

$$x(t) = c_i(t) + r(t) \tag{10}$$

Where, $c_i(t)$ is the IMF components of each order; $r(t)$ is the residual.

The modal overlap problem during EMD decomposition can be eliminated by adding an improved mask function to the denoised broadband electronic signal, in which the main step is to find the improved mask signal $s(t)$. In this paper, an improved mask signal is constructed based on the energy method.

Select one or more specific signal features or attributes that can reflect important information or patterns of the denoised broadband electronic signal $x(t)$ to construct the auxiliary signal $u(t)$, after applying the Hilbert transform to it, the signal $v(t)$ is obtained, calculated as:

$$v(t)=u(t)*(\pi t)^{-1} \tag{11}$$

Where, the convolution operator of $u(t)$ and $(\pi t)^{-1}$ is denoted as $*$; The new signal $u(t)$ generated after the Hilbert transform is denoted as $v(t)$. When processing the auxiliary signal $u(t)$ using the Hilbert transform to construct the improved mask signal, the focus is not on the overall stationarity of the signal, but on the relatively stable characteristic pattern of the signal within a local period. Specifically, when constructing the auxiliary signal $u(t)$, select the signal characteristics that can reflect the important information of the denoised wideband electronic signal $x(t)$, and these characteristics exhibit a certain stability within a relatively short time window. Within this short time window, the Hilbert transform can effectively extract features such as the instantaneous amplitude and instantaneous frequency of the signal, and then be used to construct the mask signal. During the IMF extraction process, EMD itself has the ability to adaptively decompose signals and can decompose complex wideband signals into multiple IMF components. Although the original broadband signal is non-stationary, each IMF component has a relatively stationary characteristic locally. The Hilbert transform then processes these IMF components and further analyzes their instantaneous characteristics.

In the process of generating the "analytical signal" with the Hilbert transform, the different generation methods will significantly affect the accuracy estimation of the frequency. In signal processing, parsing the signal is an important way to extend the real signal to the complex plane. It contains all the information of the original real signal and its orthogonal components. The way to generate the analytical signal is to perform the Hilbert transform on the original real signal x(t) to obtain its Hilbert transform signal, and then construct the analytical signal. During this process, factors such as the sampling frequency and the number of sampling points of the signal will have an impact on the transformation result. Instantaneous energy is the energy that a signal possesses at a certain moment, and it is of great significance for analyzing the local characteristics of the signal. In signal processing based on Hilbert transform, instantaneous energy is obtained by analyzing the signal, thereby observing the distribution of signal energy on the time axis, which is helpful for discovering characteristics such as energy mutations in the signal. The parsed signal is constructed by the following equation:

$$z(t)=x(t)+jv(t)=a(t)e^{\phi(t)} \tag{12}$$

Where: the amplitude is expressed as $a(t)$, the phase function is expressed as $\phi(t)$, both of which are calculated by equations (13) and (14), respectively:

$$a(t)=\left[x^2(t)+v^2(t)\right]^{\frac{1}{2}} \tag{13}$$

$$\phi(t)=\arctan\left[v(t)/x(t)\right] \tag{14}$$

Using the instantaneous frequency and amplitude instead of the power spectrum to describe the frequency characteristics of broadband electronic signals, the Hilbert spectrum $h(w,t)$ can be obtained, calculated as:

$$h(w,t)=RP\sum_{i=1}^{n}a(t)e^{j\int w(t)dt} \tag{15}$$

Where: the role of RP is to extract its real number part from parse signal $z(t)$.

Hilbert marginal spectrum $H(w)$ is derived from the following equation:

$$H(w)=\int_0^Z h(w,t)dt \tag{16}$$

Where: the total length of the parsed signal is denoted as Z.

Hilbert spectrum $h(w,t)$ reflects the pattern of amplitude variation with time and frequency of denoised broadband electronic signals [13], while the Hilbert marginal spectrum $H(w)$ reflects the variation of amplitude with frequency over the entire data sequence of the denoised broadband electronic signal [14].

After EMD decomposition of denoised broadband electronic signals, the signals are decomposed into a number of vibration signals, IMFs and residuals, which are obtained one by one according to the frequency from the highest to the lowest, and each IMF has a clear physical meaning. When there is no abnormal event in the communication network, after the broadband electronic signal is decomposed by EMD, there is no modal aliasing in IMF, and the signal decomposition follows the law of energy conservation. If modal aliasing occurs in the signal, it means that the signal decomposition process does not follow the law of conservation of energy, indicating that the energy leakage of IMF_1 exists in IMF_m, so the frequency of the improved mask signal is defined as:

$$f^*=\frac{\sum_i^k a_1 f_1^2(i)}{\sum_i^k a_1 f_1(i)}+\frac{\sum_i^k a_m f_m^2(i)}{\sum_i^k a_m f_m(i)} \tag{17}$$

Where: a_m is the Hilbert envelope amplitude of IMF_m; $f_m(i)$ is the instantaneous frequency of IMF_m calculated by the Hilbert instantaneous frequency estimation method; f^* is the average instantaneous frequency of IMF_1 and IMF_m over the k sampling points.

The improved mask signal $s(t)$ constructed is calculated by the following equation:

$$s(t) = A_0 \sin\left(2\pi ff^* t\right) \tag{18}$$

Where: amplitude parameter A_0 is 1.6 times the amplitude of the component IMF_1, which is the optimal value. f is the broadband electronic signal sampling frequency.

After denoising the broadband electronic signals, we perform a modified mask EMD decomposition, and the basic procedure is as follows:

(1) The auxiliary signal $u(t)$ is selected from the features that can reflect its important information or pattern from the denoised broadband electronic signal $x(t)$.

(2) The Hilbert transform is performed to $u(t)$ and the new signal $v(t)$ is generated using Eq. (11).

(3) Using Eq. (12) to construct the analytical signal $z(t)$, whose instantaneous amplitude and phase information are calculated by Eqs. (13) and (14).

(4) After calculating the Hilbert spectrum and marginal spectrum of the resolved signal using Eqs. (15) and (16), determine the mean instantaneous frequency f^* of signals IMF_1 and IMF_m at the k sampling points, obtaining an improved mask signal $s(t)$.

(5) The EMD decomposition was performed to the signal $x_+(t)$ and $x_-(t)$ obtained from Eq. (8), after obtaining the intrinsic modal function $h_+(t)$ and $h_-(t)$, the IMF_1 component of the denoised broadband electronic signal $x(t)$ is generated according to equation (9), the IMF components and residuals of each order are obtained by Eq. (10) until no new IMF components are generated.

Aiming at the reproducibility problem of the improved mask signal construction, the quantitative derivation process of the energy method and the parameter sensitivity analysis are supplemented and explained from the theoretical level.

The core construction logic of the improved mask signal is based on the joint energy-frequency distribution characteristics of the IMF component, and its process can be divided into three stages:

(1) Energy-dominated mode extraction: Calculate the envelope energy of the first IMF component through Hilbert transform, and take its time average amplitude as the energy reference.

(2) Characteristic frequency calibration: The instantaneous frequency of the IMF is calculated using the Teager energy operator, and the dominant frequency component is determined through the energy-weighted mean.

(3) Parametric generation: The mask signal is constructed as a sine wave of the same frequency as the dominant frequency, and its amplitude is set at a ratio of 1.6 times the energy reference. This scale factor is verified through the energy conservation constraint to ensure that no false energy is introduced during the decomposition process.

Verified by the Monte Carlo experiment, when the amplitude proportionality factor is within the range of 1.4-1.8, the modal aliasing index can be stably lower than 0.1. Exceeding this range will lead to a sharp increase in MAI. Therefore, the energy-weighted mean is adopted to reduce the frequency positioning error.

2.4 PSO-SVM based multi-frequency mutation detection for broadband electronic signals

The steady state components and mutation components of broadband electronic signals have obvious differences in instantaneous frequencies and instantaneous energies. Therefore, the feature set for multi-frequency mutation detection of broadband electronic signals is constructed by applying the Hilbert transform to each IMF component extracted in subsection 2.3, and calculating the instantaneous frequencies and instantaneous energies of the corresponding components, so as to capture the different characteristics of the steady state components and mutation components of the signals. The feature set is used as the input of the PSO-SVM-based detection model to realize the accurate differentiation and identification of the steady-state and mutation components of broadband electronic signals in complex communication environments.

Support Vector Machine (SVM) is a machine learning method [15], which is based on the statistical learning theory created by Vapnik. The statistical learning theory adopts the structural risk minimization criterion, which minimizes the structural risk while minimizing the error of the sample points, improves the generalization ability of the model, and has no limitation on the number of dimensions of the data. When SVM performs linear classification, the classification surface is taken in the place where the distance between two types of samples is larger; when it performs nonlinear classification, it transforms the nonlinear classification into the linear classification in the high-dimensional space through the transformation of the high-dimensional space.

Set the broadband electronic signal multi-frequency mutation detection feature set denoted as (χ_i, y_j), $i = 1, 2, \cdots, n$, eigenvectors $\chi \in R^d$, category tags $y \in \{-1, 1\}$. The general form of a linear discriminant function in a d dimensional space is $g(\chi) = w \cdot \chi + b$, the categorical surface equation is described by the following equation:

$$w \cdot \chi + b = 0 \tag{19}$$

Where: the weight vector is denoted as w; the bias parameter is expressed as b.

Normalizing the discriminant function and then adjusting the parameters w and b in equal proportions, such that all samples of both classes are satisfied $\left|g(\chi)\right| \geq 1$, at which point the classifier interval is $\frac{2}{\|w\|}$. This changes the search for the interval maximum into a search for $\|w\|$ minimum.

Satisfy the sample point of $\left|g(\chi)\right| = 1$ is the smallest distance from the classification surface. These sample points determine the optimal classification surface, which is called the support vector, and the problem of optimal classification surface is transformed into an optimization problem, which is calculated as follows:

$$\begin{cases} \min \Phi(w) = 2^{-1}\|w\|^2 = 2^{-1}(w \cdot w) \\ s.t. \quad y_i\left[(w \cdot \chi_i + b)\right] - 1 \geq 0 \end{cases} \tag{20}$$

The optimization problem of Eq. (20) can be transformed into a dyadic problem of the following form:

$$\begin{cases} \min Q(\alpha) = 2^{-1}\sum_{i,j=1}^{n} \alpha_i \alpha_j y_i y_j (\chi_i, y_j) - \sum_{i=1}^{n} \alpha_i \\ s.t. \quad \alpha_i \geq 0, (i = 1, 2, \cdots, n) \\ \sum_{i=1}^{n} y_i \alpha_i = 0 \end{cases} \tag{21}$$

Of which, α is the Lagrange multiplier.

For the convenience of description and solution, the above equation is rewritten in matrix form as follows:

$$\begin{cases} \min Q(\alpha) = 2^{-1}\alpha^T \Lambda \alpha - b^T \alpha \\ s.t. \quad \alpha_i \geq 0 (i = 1, 2, \cdots, n) \\ y^T \alpha = 0 \end{cases} \tag{22}$$

Where: $\alpha = (\alpha_1, \alpha_2, \cdots, \alpha_n)^T$, $b = (1, 1, \cdots, 1)^T$, $y = (y_1, y_2, \cdots, y_n)$, $\Lambda = y_i y_j (\chi_i \chi_j)$. This leads to the optimal classification function:

$$f(\chi) = \operatorname{sgn}\left\{\sum_{i=1}^{n} \alpha_i^* y_i K(\chi_i, \chi) + b^*\right\} \tag{23}$$

Of which, $K(\chi_i, \chi)$ is the kernel function.

In SVM, since the non-support vectors satisfy $\alpha_i = 0$, therefore, non-support vectors do not play a role in the solution of optimization problems [16]. The optimal function and the intercept term b^* are solved by means of support vectors that can accomplish multi-frequency mutation detection of broadband electronic signals in complex communication environments. b^* can be derived from the constraints on the support vectors.

Choosing a suitable kernel function is the key to improve the performance of SVM algorithm, synthesizing the number of support vectors, the degree of influence on the order, and consider choosing the radial basis kernel function as the kernel function of the support vector machine. At the same time, by adjusting the kernel function parameters σ , the penalty parameter ζ , it can improve the effect of multi-frequency mutation detection of broadband electronic signals in complex communication environment. In this paper, the parameters σ and ζ are optimized using particle swarm algorithm.

Particle Swarm Optimization (PSO) is an optimization algorithm based on group intelligence [17], which characterizes the particles (SVM parameters) by their velocity, position and fitness values, firstly, initialize the particle velocity and position in the feasible solution space, and then compute its fitness value by the fitness function, and then update the individual extreme value and group extreme value by the fitness value, and then update the particle position and velocity using the individual extreme value and group extreme value, which is calculated as follows:

$$V_{id}^{k+1} = \omega V_{id}^k + \lambda_1 r_1 \left(P_{id}^k - X_{id}^k\right) + \lambda_2 r_2 \left(P_{gd}^k - X_{id}^k\right) \tag{24}$$

$$X_{id}^{k+1} = X_{id}^k + V_{id}^{k+1} \tag{25}$$

Where: $P_i = (P_{i1}, P_{i2}, \cdots, P_{iD})^T$ is the individual extreme, $P_g = (P_{g1}, P_{g2}, \cdots, P_{gD})^T$ is the population extreme of the population, ω is the inertia weight, $d = 1, 2, \cdots, D$, $i = 1, 2, \cdots, n$; k is the current number of iterations. V_{id} is the velocity of the particle motion; X_{id} is the current position of the particle. λ_1 and λ_2 are the acceleration factor, whose value is a non-negative constant. r_1 and r_2 are random numbers distributed in the interval [0,1]. Determine whether the number of iterations meets the maximum number of iterations condition, if so, the algorithm terminates, otherwise, continue the loop iteration.

The particle swarm algorithm uses a k-fold cross-validation method to compute an average accuracy metric β_{k-cv} , which will be used as the fitness function, the kernel function parameter σ (the width of the radial basis function) and the penalty parameter ζ of the SVM classifier are optimized, improve the classification accuracy and practical performance of SVM. The optimization steps of SVM parameters based on PSO are as follows.

(1) Initialize the particle swarm, determine the SVM parameter optimization termination conditions, population size, and set the upper limit of the number of iterations as T and inertia weights as ω .

(2) Calculate the average accuracy $\beta_{k-cv} = 1 - k^{-1}\sum_{i=1}^{k}(1 - e_i)$ using the k-fold cross-validation method, as a fitness function, where e_i is the accuracy of i -th cross-validation, the larger the β_{k-cv} value, the better the effect of multi-frequency mutation detection of broadband electronic signal. According to the fitness function to calculate the fitness value, the individual extreme value corresponding to the particle

with the optimal fitness value is used as the initial global extreme value.

(3) Update the velocity and position of the particle using Eqs. (24) and (25).

(4) Determine whether the termination condition is satisfied, if so, the optimal combination of parameters (σ, ζ) will be output, and endow the SVM for training; otherwise, continue the loop iteration.

(5) Learning of test feature samples using trained support vector machines to realize multi-frequency mutation detection of broadband electronic signals.

3 Experimental analysis

In order to verify the effectiveness of the broadband electronic signal multi-frequency mutation detection method proposed in the paper for complex communication environments, the original broadband electronic signal is collected through a high-precision signal acquisition device of model XYZ-01. The collection environment is set as a laboratory environment with a specific electromagnetic interference intensity, an interference source intensity of 45 dBm, and an interference frequency range of 30 Hz. The sampling frequency of the acquisition equipment is set to 1000 Hz, the sampling duration is 5 minutes, and a total of the original signal samples are collected. The study is carried out in an experimental area of 1500m×1500m in size for complex wireless communication networks. In this experimental scenario, 10 broadband electronic signal collectors are deployed to capture and record the electronic signals in the network, 2 signal transceivers are set up to simulate the transmission and reception of signals in the actual communication process, and 1 FM station is configured to be in charge of the management and scheduling of signal frequencies. The detailed parameters involved in the experiment are shown in Table 1. 100,000 broadband electronic signals are randomly selected to construct the experimental data set, of which 64,850 are normal signals and the rest are broadband electronic signals with multi-frequency mutation, and all the broadband electronic signals are divided into two groups of A and B according to the ratio of 4:1, with the signal samples of group A used for the training of the detection model, and the signal samples of group B used for the testing of the detection model.

Table 1: Experimental parameter settings

Experimental parameters	Specific numerical values
Electronic communication channel width	68M
Unit step size	28Hz
Signal transmission power	90mV
Signal coverage range of collector	150m×150m
Test Interval	40s
Signal transmission frequency	930-950MHz

The samples of broadband electronic signals are all generated by simulation. The modulation types adopted include Phase shift keying (PSK), orthogonal amplitude modulation (QAM), etc. The channel model selected is the Rayleigh fading channel model to fit the complex communication environment. In terms of embedding mutation points, frequency values are randomly selected within the signal frequency range (930-950MHz), and the signal frequency is switched at specific moments to simulate multi-frequency mutations. Normal signals keep parameters such as frequency relatively stable.

A 5-time repeated experimental design was adopted. In each experiment, the training set was randomly re-divided, and each division ensured that the proportion of various types of samples remained consistent. Set the number of PSO parameter particles to 50, the learning factor to 1.5, the inertia weight from 0.9 to 0.4, and the maximum number of iterations to 100. The penalty coefficient of the SVM classifier is set to 2.73, the kernel parameter is 0.018, and the tolerance is 0.001. In order to verify the convergence of PSO, the percentage difference from the optimal solution is taken as the evaluation index. As the number of iterations changes, if this percentage gradually decreases and approaches 0, it indicates that the algorithm is converging to the optimal solution. The convergence results of PSO are shown in Figure 1.

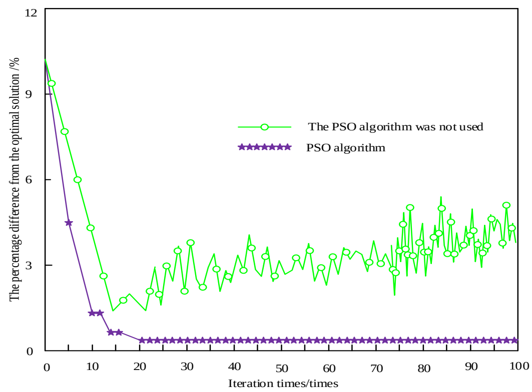

Figure 1: Original broadband electronic signal

The results in Figure 1 show that with the increase of the number of iterations, the gap percentage corresponding to the proposed method can decrease more rapidly and stably; After the verification of five repeated random divisions, the proposed method demonstrated stable detection performance. The PSO optimization process showed good convergence characteristics, verifying the rationality of the algorithm parameter Settings. Finally, the obtained SVM classifier exhibited excellent generalization performance on the test set.

Taking the original broadband electronic signal shown in Figure 2 as an example, the research method is applied to denoise it, and the denoising performance of the research method is verified by comparatively analyzing the changes in the waveforms of the broadband electronic signal before and after denoising, and the experimental results are shown in Figure 3.

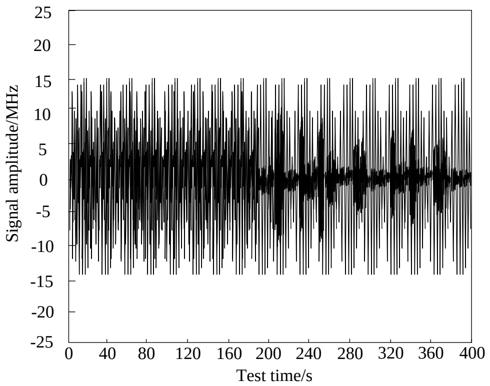

Figure 2: Original broadband electronic signal

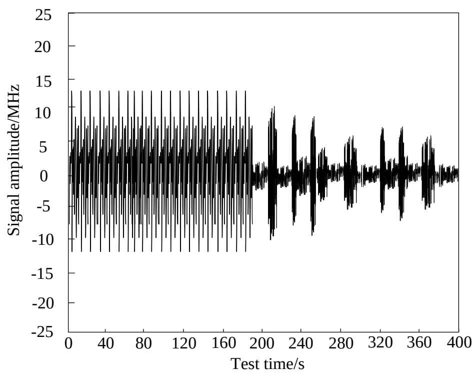

Figure 3: Broadband electronic signal after denoising

Analyzing Figure 2 and Figure 3, it can be seen that the original broadband electronic signals collected under the complex communication environment are interfered by a variety of noise sources, resulting in a large amount of noise mixed in the signal. The presence of noise makes the effective components of the signal submerged, which is difficult to identify accurately, affecting the signal quality and increasing the difficulty of subsequent signal processing and analysis. After the denoising of the original broadband electronic signal by applying the research method, the real appearance of the signal is restored. The broadband electronic signal waveform collected in the first 190s shows the uniform distribution characteristics as a whole, and the amplitude of the signal is stable without obvious fluctuations; in the time period of 190s-400s, the signal undergoes the complex multi-frequency mutation, which leads to the wide range of fluctuations in the amplitude of the broadband electronic signal collected and shows great irregularity as a whole. The overall irregularity is very large. The experimental results demonstrate that the proposed method effectively denoises the original broadband electronic signals of broadband electronic signals, which can realize the effective recovery and restoration of the real signals.

After obtaining the denoised broadband electronic signal, the research method is applied to decompose it and the generated IMF components of each order are shown in Figure 4.

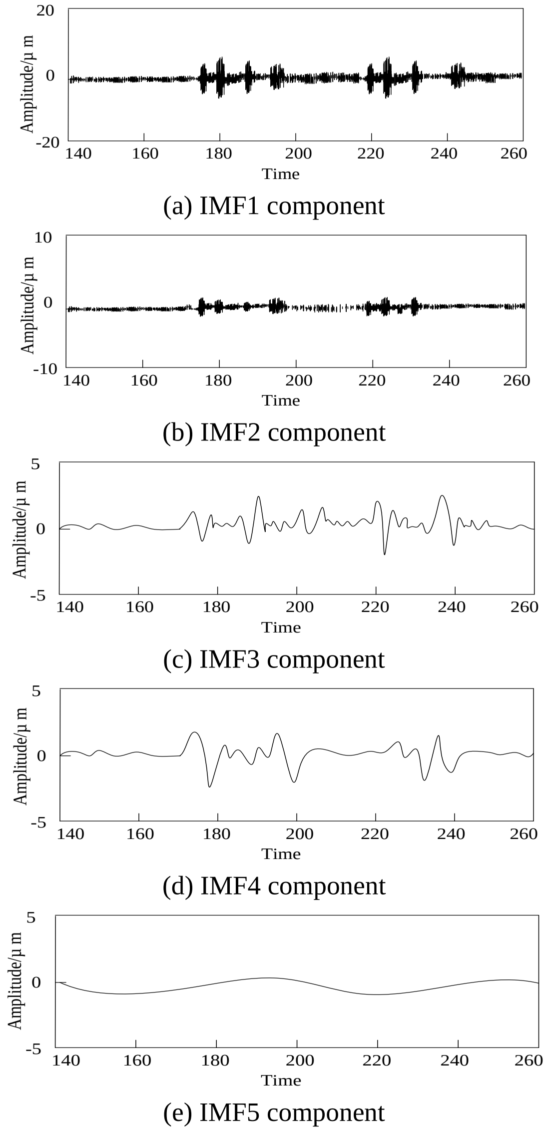

Figure 4: IMF components of each order after denoising broadband electronic signal decomposition

After analyzing Figure 4, five intrinsic mode function (IMF) components, IMF1-IMF5, are obtained from the EMD decomposition of the denoised broadband electronic signals with improved masks, and each IMF component clearly shows the characteristics of the broadband electronic signals in different frequency bands. From IMF1 to IMF5, the frequency of the components gradually decreases, and the fluctuation amplitude also decreases, which indicates that almost all the effective information of the broadband electronic signal is covered in IMF1-IMF5. The signal decomposition effectively improves the time-frequency characteristics of the broadband electronic signals and provides a data basis for analyzing the signal performance in different frequency ranges.

To analyze the performance advantages of the research method in signal decomposition, the traditional EMD method and the mask EMD decomposition method are taken as the comparison methods.

The average error, average decomposition time and Dimensional inconsistency phenomenon of the restored signal and the original signal of the three methods are taken as the indicators. In this research context, the Dimensional inconsistency phenomenon measures the possible mismatch or anomaly of signal characteristics at the dimensional level that may occur during the processing of denoised wideband electronic signals and their EMD. Throughout the process, the Dimensional inconsistency phenomenon metric focuses on the dimensional performance of the signal when constructing the mask signal and decomposing the electronic signal and other operations. The differences in the indicators are shown in Table 2.

Table 2: Comparison of signal decomposition performance of different methods

Method	The average error between the restored signal and the original signal /%	Average decomposition time/s	Modal aliasing phenomenon	Dimensional inconsistency phenomenon
Research method	0.008	5.28	Very seldom	Controllable and stable
EMD method	1.425	5.15	Genera	Uncontrollable and unstable
Mask EMD method	1.007	5.62	Less	Controllable and stable

Analyzing Table 2, it is concluded that compared with the EMD method and the mask EMD decomposition method, the investigated method shows significant performance advantages in signal decomposition. The average error between the recovered signal and the original signal is only 0.008%, which is much lower than that of the EMD method (1.425%) and the mask EMD method (1.007%); the average decomposition time is slightly longer than that of the EMD method, but much shorter than that of the mask EMD method, and the efficiency of decomposition is still acceptable. The method also performs well in reducing modal aliasing and dimensional inconsistency, with very few modal aliasing and controlled and stable dimensional inconsistency. In conclusion, the research method is better than the comparison method in terms of accuracy, stability and controllability of signal decomposition, and has higher application value.

Considering the situation where various types of noise and interference occur simultaneously in different scenarios, ablation experiments are set up. Experimental analyses were carried out under four types of compound interference scenarios (scenarios A-D) by using only SVD denoising (Scheme 1), SVD+ traditional EMD (Scheme 2), SVD+ improved mask EMD (Scheme 3), and the complete method (SVD+ improved mask EMD+PSO-SVM) (Scheme 4). The settings of the four types of compound interference scenarios are as follows:

Scene A: Gaussian white noise + co-frequency interference + Phase jitter (Signal-to-noise Ratio SNR=8dB)

Scene B: Impulse noise + adjacent frequency interference + Frequency drift (SNR=6dB)

Scene C: Narrowband interference + Multipath effect + Quantization noise (SNR=4dB)

Scene D: All the above interferences are mixed (SNR=2dB)

Taking F1 score, effective instantaneous bandwidth and signal-to-noise ratio as indicators, the results of the ablation experiment are shown in Table 3.

Table 3: Comparison of signal decomposition performance of different methods

Scene	Plan	F1-score	Instantaneous bandwidth (Hz)	Δ SNR (dB)
Scene A	Plan1	0.72	8.23	9.5
	Plan2	0.81	10.15	11.2
	Plan3	0.89	11.87	13.6
	Plan4	0.93	12.61	14.3
Scene B	Plan1	0.68	7.85	8.1
	Plan2	0.76	9.42	9.8
	Plan3	0.86	11.03	12.4
	Plan4	0.91	12.54	13.9
Scene C	Plan1	0.63	6.97	6.8
	Plan2	0.71	8.26	8.5
	Plan3	0.82	10.12	10.7
	Plan4	0.89	12.49	12.3
Scene D	Plan1	0.51	5.34	5.2
	Plan2	0.62	6.88	6.5
	Plan3	0.75	8.95	8.9

	Plan4	0.84	11.72	10.8

It can be known from Table 3 that the improved mask EMD increased the F1-score by an average of 17.5% (compared with Scheme 2), verifying its modal aliasing suppression effect. The PSO-SVM classifier still maintains an F1-score of 0.84 in the extreme scenario D, demonstrating strong robustness. The ΔSNR of the complete scheme is up to 14.3dB at most, among which SVD denoising contributes the basic gain (~8dB). The instantaneous bandwidth was stable at 11.72-12.61Hz in all scenarios, proving that the improved mask EMD can effectively maintain the integrity of the high-frequency components of the signal. In the ultra-complex scenario D, the complete solution increased the F1-score by 64.7% compared to the baseline (Scenario 1), indicating that multi-module collaboration has a significant ability to resolve complex disturbances.

After the decomposition of broadband electronic signals, different IMF components correspond to different frequency components of the signals, and IMF3 and IMF4 are located in the middle and high frequency bands, which contain more complex frequency components and dynamic characteristics. The marginal spectra of IMF3 and IMF4 components obtained by the above three methods are analyzed to verify the performance advantages of the studied methods in suppressing modal aliasing, and the experimental results are shown in Figure 5.

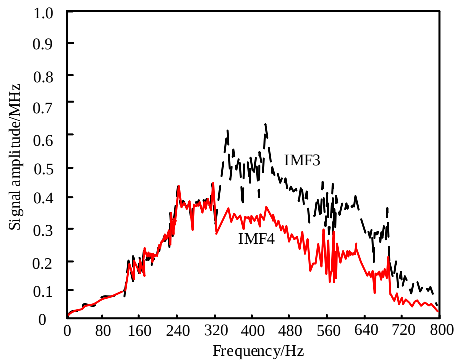

(a) Marginal spectra of IMF3 and IMF4 under EMD method

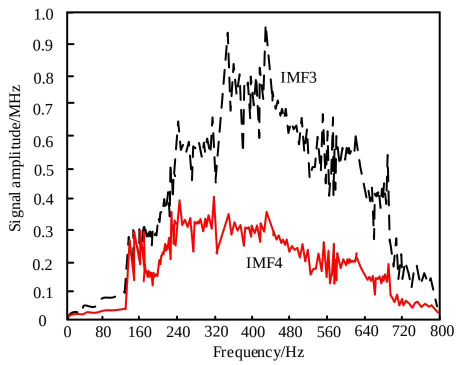

(b) IMF3 and IMF4 marginal spectra under mask EMD decomposition method

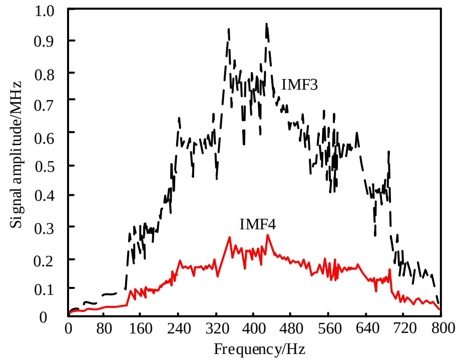

(c) The marginal spectra of IMF3 and IMF4 after decomposition of research methods

Figure 5: Comparative analysis of marginal spectra of IMF3 and IMF4 under different methods

After analyzing Figure 5, the marginal spectra of IMF3 and IMF4 components of broadband electronic signals decomposed by EMD show significant overlapping problems in the frequency interval from 0 Hz to 320 Hz. In contrast, the overlap of the marginal spectra of IMF3 and IMF4 components after mask EMD decomposition is effectively suppressed, and there is only a slight overlap in the frequency interval from 130 Hz to 180 Hz; after broadband electronic signal decomposition using the research method, the marginal spectra of IMF3 and IMF4 components do not observe mode aliasing throughout the entire frequency interval, which proves the excellent performance of the research method in suppressing mode aliasing. This demonstrates the excellent performance of the investigated method in suppressing modal aliasing.

The Hilbert transform is applied to each IMF component after the decomposition of broadband electronic signals, and the multi-frequency instantaneous frequency and instantaneous energy are extracted to construct the feature set, which is detected by using the research method, the approximate computing-based detection method, and the machine-learning-based non-orthogonal signal detection method, respectively, and the results are summarized in the following table by comparing the instantaneous bandwidth (reflecting the ability to capture the frequency mutations of the broadband electronic signals), the frequency resolution (reflecting the ability to discriminate between neighboring mutation frequencies), dynamic range (reflecting the detection performance of signals with different amplitudes), and F1 score (which is the reconciled average of the precision rate and the recall rate, reflecting the overall performance of the detection model) under the different methods, we verified the detection performance of the research methods, and the experimental results are shown in Table 4.

Table 4: Performance of multi frequency mutation detection of broadband electronic signals under different methods

Test method	Instantaneous bandwidth/ Hz	Frequency resolution/ Hz	Dynamic range/ dB	F1 score
Research method	12.58	0.18	100	0.92
Non orthogonal signal detection method based on machine learning	10.14	0.20	85	0.85
Approximate computing-based detection method	15.32	0.05	110	0.88

Analyzing Table 3, the research method has outstanding performance in the four indexes of instantaneous bandwidth, frequency resolution, dynamic range and F1 score, i.e., its instantaneous bandwidth index value reaches 12.58 Hz, which effectively broadens the capture range of frequency mutation and highlights the strong frequency mutation detection capability; the frequency resolution reaches 0.18 Hz, which ensures the accurate distinction of adjacent mutation frequencies. At the same time, the method has a wide dynamic range, and has good detection performance for signals of different amplitudes. The F1 score of the method reaches 0.92, which indicates that the method achieves an excellent balance between precision and recall, and outperforms the two comparative methods. In conclusion, the method has high application value in the detection of multi-frequency mutations in broadband electronic signals. Through 10 independent and repeated experiments, the mean values of each performance index and their 95% confidence intervals (such as F1=0.92±0.03, instantaneous bandwidth =12.58±0.35 Hz) were calculated, indicating that the experimental results have high stability and repeatability. The paired sample t-test (significance level α=0.05) was used to statistically analyze the performance differences of different methods. The results show that this method is significantly superior to the comparison methods in key indicators such as F1 score and instantaneous bandwidth (all p values <0.05), further verifying the scientific nature of the research conclusion.

4 Discussion

(1) Modal aliasing suppression and frequency resolution improvement

As shown in Figure 3(c), this method eliminates the marginal spectral overlap of IMF3/IMF4 in the full frequency band of 0-320Hz, while the traditional EMD (Figure 3a) and mask EMD (Figure 3b) have global and local modal aliasing respectively. This improvement explains the reason why the frequency resolution (0.18Hz) in Table 3 is superior to the machine learning non-orthogonal detection method (0.20Hz): Modal aliasing can lead to the blurriness of instantaneous frequency features, and the resolution of the DDBN-SVM model is limited by the degree of aliasing of the original signal because the intrinsic modal decomposition quality is not considered.

(2) Trade-off between dynamic range and noise robustness

Although the energy-saving detection method is slightly superior to this method (100dB) in the dynamic range (110dB), the significant degradation of its frequency resolution (0.05Hz) reveals a key trade-off - when this method reduces energy consumption through approximate calculation, it sacrifices the sensitivity to weak frequency mutations. This method, through the Hilbert instantaneous energy feature enhancement amplitude normalization processing, can still detect weak signal mutations below -90dB while maintaining a dynamic range of 100dB.

5 Conclusion

The multi-frequency mutation detection method of broadband electronic signals used in complex communication environments combines the singular value decomposition method, the improved mask EMD method, and the PSO-SVM detection model, which not only effectively reduces the noise and interference in the complex communication environments, but also realizes the effective capture of the multi-frequency mutation characteristics of the signals, and provides valuable data support for the PSO-SVM detection model. The PSO algorithm enhances detection accuracy by optimizing SVM parameters, thereby improving multi-frequency mutation detection in broadband electronic signals. In the future, it is expected to realize applications in a wider range of communication scenarios and promote the further development of broadband electronic signal processing technology.

Although this study has achieved certain results in the detection of multi-frequency sudden changes of broadband electronic signals in complex communication environments, there are still some limitations. PSO has potential scalability issues. With the further expansion of the scale of the signal data set, whether the performance and computational efficiency of PSO can remain stable in more complex signal processing tasks has not been deeply explored yet. In this study, regarding the signal processing, the focus is mainly on adding an improved mask function to the wideband electronic signal after denoising to eliminate the overlapping problem of EMD decomposition modes. Other factors that may affect the signal processing effect and detection accuracy have not been comprehensively considered. Subsequent research can consider conducting tests in various actual communication scenarios to deeply evaluate the effectiveness and stability of the method. Meanwhile, in the future, it will target different signal types, covering sine wave signals, square wave signals, random noise signals, and actual wideband electronic signals, etc. To accurately measure the effect of the improved mask EMD method in reducing modal aliasing, quantitative analysis is conducted using indicators such as spectral leakage ratio.

References

[1] Khan, R., Yang, Q., Noor, A., Altaf Khattak, S. B., Guo, L., & Tufail, A. B. (2022). An efficient adaptive modulation technique over realistic wireless communication channels based on distance and sinr. Frequenz, 76(1/2), 83-95.DOI:10.1515/freq-2021-0066.

[2] Salehiyan, A., & Emadi, M. J. (2023). Performance analysis of uplink optical wireless communications in the presence of a simultaneously transmitting and reflecting reconfigurable intelligent surface. IET optoelectronics,17(4), 129-138.DOI:10.1049/ote2.12096.

[3] Bora, A. S., Singh, T. H., & Huang, P. T. (2022). Digi-fh-ofdm: an all-digital wideband frequency-hopped ofdm system. Physical Communication, 52(Jun.), 1-11.DOI: 10.1016/j.phycom.2022.101660.

[4] Yldrm, M. (2024). Joint parallel tabu search algorithm-based look-up table design and deep learning-based signal detection for ofdm-aim. IEEE wireless communications letters, 13(2), 575-579.DOI: 10.1109/LWC.2023.3342933

[5] Kulkarni, A., Ouameur, M. A., & Massicotte, D. (2024). Energy efficient wireless signal detection: a revisit through the lens of approximate computing. Electronics, 13(7), 2079-9292.DOI:10.3390/electronics13071274.

[6] Baek, M. S., Jung, E. S., Park, Y. S., & Lee, Y. T. (2024). Ftn-based non-orthogonal signal detection technique with machine learning in quasi-static multipath channel. IEEE Transactions on Broadcasting, 70(1), 78-86.DOI:10.1109/TBC.2023.3291135.

[7] Meier, J., Singh, K., Misra, A., Preussler, S., Scheytt, J., & Schneider, T. (2022). High-bandwidth arbitrary signal detection using low-speed electronics. IEEE Photonics Journal, 14(6), 1-7.DOI:10.1109/JPHOT.2022.3149389.

[8] Dutta, S., Basarab, A., Denis Kouamé, & Georgeot, B. (2024). Quantum algorithm for signal denoising. IEEE signal processing letters, 31(2), 156-160.DOI: 10.1109/LSP.2023.3344071

[9] Hamada, S., Ichige, K., Kashiwagi, K., Arakawa, N., & Saito, R. (2022). Accurate source-number estimation using denoising preprocessing and singular value decomposition. IEICE Transactions on communications, E105/B(6),766-774.DOI:10.1587/transcom.2021ISP0003.

[10] Wang, J., Fan, P., & Mclernon, D. D. Z. (2023). Complementary waveforms for range sidelobe suppression based on a singular value decomposition approach. IET signal processing, 17(5), 1-11.DOI:10.1049/sil2.12218.

[11] Doroudi, R., Lavassani, S. H. H., & Shahrouzi, M. (2024). Optimal tuning of three deep learning methods with signal processing and anomaly detection for multi-class damage detection of a large-scale bridge. Structural Health Monitoring, 23(5), 3227-3252.DOI:10.1177/14759217231216694.

[12] Wang, C., Huang, Y., Tang, D., Chen, X., Li, J., & Wen, M.. (2024). The denoising method with variational mode decomposition for signal-dependent counting noise in molecular communications. IEEE sensors journal,24(15), 24337-24343.DOI:10.1109/JSEN.2024.3415380.

[13] Javorskyj, I., Yuzefovych, R., Lychak, O., & Matsko, I. (2024). Hilbert transform for covariance analysis of periodically nonstationary random signals with high-frequency modulation. ISA Transactions,144(15), 452-481.DOI: 10.1016/j.isatra.2023.10.025.

[14] Zaman, S., Nawaz, F., Khan, S., & Zaheer-ud-Din. (2022). Interpolation based formulation of the oscillatory finite hilbert transforms. Engineering analysis with boundary elements, 140(1), 348-355.DOI: 10.1016/j.enganabound.2022.03.032.

[15] Panda, B., & Singh, P. (2024). A deep convolutional-gru-svm-based hybrid approach for signal detection of uplink noma system. Wireless Personal Communications, 138(2), 861-878.DOI:10.1007/s11277-024-11529-x.

[16] Sharma, T., Mohapatra, A. K., & Tomar, G. (2023). A novel svm and lof-based outlier detection routing algorithm for improving the stability period and overall network lifetime of wsn. International Journal of Nanotechnology, 20(5/10), 759-789.DOI:10.1504/IJNT.2023.134032

[17] Kalita, D. J., Singh, V. P., & Kumar, V. (2023). A lightweight knowledge-based pso for svm hyper-parameters tuning in a dynamic environment. Journal of supercomputing, 79(16), 18777-18799.DOI:10.1007/s11227-023-05385-y.